Leaf reflectance can surrogate foliar economics better than physiological traits across macrophyte species

Paolo Villa[1,*], Rossano Bolpagni[1, 2], Monica Pinardi[1], Viktor R. Tóth[3,*]

[1] *Institute for Electromagnetic Sensing of the Environment, National Research Council of Italy (CNR-IREA), Milan (Italy)*

[2] *Department of Chemistry, Life Sciences and Environmental Sustainability, University of Parma, Parma (Italy)*

[3] *Balaton Limnological Institute, Centre for Ecological Research, Tihany (Hungary)*

***corresponding authors:** villa.p@irea.cnr.it (P. Villa); toth.viktor@okologia.mta.hu (V. R. Tóth)

Abstract

Macrophytes are key players in aquatic ecosystems diversity, but knowledge on variability of their functional traits, among and within species, is still limited. Remote sensing is a high-throughput, feasible option for characterizing plant traits at different scales, provided that reliable spectroscopy models are calibrated with congruous empirical data.

We sampled leaves from six macrophyte species common in temperate areas, covering different phenological stages, seasons, and environmental conditions, and measured leaf reflectance (400-2500 nm) and traits (dealing with photophysiology, pigments and leaf economics). We explored optimal spectral bands combinations and established non-parametric reflectance-based models for selected traits, eventually showing how airborne hyperspectral data can capture spatial-temporal macrophyte variability.

Our key finding is that structural, leaf dry matter content, leaf mass per area (LMA), and biochemical, chlorophyll-a content and chlorophyll to carotenoids ratio, traits can be surrogated by leaf reflectance with relative error under 20% across macrophyte species, while performance of reflectance-based models for photophysiological traits depends on species.

This finding shows the link between leaf reflectance and structural-biochemical traits for aquatic plants, thus supporting the use of remote sensing for enhancing the level of detail of macrophyte functional diversity analysis, to intra-site and intra-species scales.

Keywords: aquatic plants; chlorophyll-a; functional traits; intraspecific variability; photophysiology parameters; leaf economics spectrum (LES); remote sensing; spectroscopy

1. Introduction

Ecotones laying at the interface between land and inland waters are among the most important (Mitra *et al.*, 2005; Tranvik *et al.*, 2009; Mitsch *et al.*, 2013), most productive (Bridgham *et al.*, 2006) and most diverse (Keddy *et al.* 2009) ecosystems in temperate areas. The origin of its exceptional diversity is attributed to its transitional status, connecting two biomes, aquatic and terrestrial (Wetzel, 1990).

Most of the diversity in these ecosystems comes from the high spatial and temporal variability of environmental conditions that creates a number of microhabitats (Spence, 1982). Within this frame, aquatic plants, i.e. macrophytes, are key players, as they are hotspots of biogeochemical cycling, actively impact on ecosystem by regulating water flow and sedimentation, and promote biodiversity by attracting and sheltering large number of species (Schindler & Scheuerell, 2002; Franklin *et al.*, 2008; Jeppesen *et al.*, 2012; Wang *et al.*, 2017). Adaptations to environmental heterogeneity is particularly evident for macrophytes, whose genetic variability and morpho-functional plasticity result in specific phenotypic and phenological patterns within the local population, shaping communities (Elzinga *et al.*, 2007; Chuine, 2010; Tóth & Szabó, 2012; Tóth & Vári, 2013) and even individuals (de Kroon *et al.*, 2005; Tóth & Palmer, 2016).

As multi-dimensional trait variability is a recent object of investigation in functional ecology (Messier *et al.*, 2010; Hu *et al.*, 2015; Butler *et al.*, 2017), knowledge about ranges and interconnections of phenotypic and phenological variability within a community (population) is still relatively limited, all the more when aquatic plants are considered, due to their peculiar features and the environmental patchiness of their habitat, showing high abiotic and biotic variability (Vivian-Smith, 1997). The issue of disentangling the effects of inter-specific and intra-specific trait variability is at the centre of the current debate (Albert *et al.*, 2012; Niinemets, 2015; Osnas *et al.*, 2018), especially for key traits related to the leaf economics spectrum (LES; Wright *et al.*, 2004). Moreover, spatial patterns of trait variability at local scale have been studied only by a limited number of works (Kumordzi *et al.*, 2015; Sandel & Low, 2019) and some light has still to be shed on this level of heterogeneity in plant communities, with implications on productivity and connected processes (Funk *et al.*, 2016; Ji *et al.*, 2020).

Exploring this fine scale variability with direct measurements, usually carried out *in situ* and in laboratory, is very time and resource consuming, and often logistically constrained in aquatic systems. The level of maturity in platforms and techniques achieved by remote sensing (RS) make it a feasible and potentially very effective way forward in characterizing selected plant trait variability within communities at different geographic scales (Asner *et al.*, 2015; Abelleira Martinez *et al.*, 2016; Gamon *et al.*, 2019), overcoming logistic and economic constraints.

In particular, the last two decades have seen the development of a range of applications for RS of plant bio-physical and bio-chemical traits, with an intensification of this trend in last decade (Homolová *et al.*, 2013; Verrelst *et al.*, 2015; Wang & Gamon, 2019). RS-based works have by a large majority focused on terrestrial plants, from forest and grassland biomes (e.g Asner & Martin, 2008; Asner *et al.*, 2015; Singh *et al.*, 2015; Schweiger *et al.*, 2017; Serbin *et al.*, 2019), but some recent developments on aquatic vegetation have been

recently documented (Stratoulias *et al.*, 2015; Villa *et al.*, 2017). For being effective, applications of RS for functional ecology require an analysis of which plant traits can be modelled from spectral reflectance, and this is preferably done using data covering natural trait heterogeneity. Empirical approaches for assessing reflectance spectra as proxy of plant traits, at leaf or canopy level, employ spectroscopy methods ranging from parametric regression models input with spectral indices, computed as band combinations (e.g. Le Maire *et al.*, 2008; Yao *et al.*, 2010; Ali *et al.*, 2017) to non-parametric regression models, such as partial least-square regression (e.g. Asner & Martin, 2008; Feilhauer *et al.*, 2010; Asner *et al.*, 2014; Meacham-Hensold *et al.*, 2020).

Towards this direction, the basilar question is: which functional traits, within a specific plant group, can be reliably modelled (and which other cannot) using spectroscopy? With this study, we aim to provide an answer to this question for what concerns floating and emergent aquatic plants common in temperate areas, based on empirical data of leaf spectra and a set of leaf traits - dealing with photophysiology, pigments and leaf economics – collected *in situ* from six macrophyte species, under different times, seasons and environmental conditions, over three sites located in Europe.

The objectives of this work are: i) to assess the variability in leaf functional traits within and among macrophyte species, with attention to autochthonous *vs.* allochthonous taxa dualism; ii) to evaluate which functional traits – photophysiological, biochemical and structural – can be effectively modelled across macrophyte species using leaf reflectance, and which wavelength ranges and combinations are more sensitive to specific traits; and iii) to test how leaf reflectance-traits relations can be exploited using remote sensing data for providing information on spatial and temporal functional variability of macrophyte communities at inter- and intra-species level.

2. Materials and Methods

2.1. Sampling site descriptions

Macrophyte samples were collected from three temperate shallow lakes surrounded by wetlands and hosting abundant macrophyte communities, located in central and southern Europe: Lake Hídvégi (Hungary), Mantua lakes system (Italy), and Lake Varese (Italy).

Lake Hídvégi, located in western Hungary (46°38′ N, 17°08′ E; 110 m a.s.l.), is an artificial lake system built in 1985 as a part of the Kis-Balaton Water Protection System, that has the overall function of retaining inorganic nutrients and total suspended solids carried by the Zala River into Lake Balaton (Korponai *et al.*, 2010). Lake Hídvégi is a shallow, eutrophic to hypertrophic, predominantly open-water habitat (area: 18 km^2, average depth: 1.1 m) partly covered by floating macrophytes, with *Trapa natans* L. as dominant species and some presence of *Nuphar lutea* (L.) Sm. and *Nymphaea alba* L. (Dinka *et al.*, 2008; Villa *et al.*, 2017). Helophyte communities in the littoral zone are composed of reed beds (*Phragmites australis* (Cav.) Trin. ex Steud.) and cattail beds (*Typha* spp.).

Mantua lakes system, located in northern Italy plain (45°10′ N, 10°47′ E; 15 m a.s.l.), is composed by three dimictic shallow fluvial-lakes (area: 6.1 km^2; average depth: 3.5 m), with two connected wetlands (upstream and downstream of lakes). The Superior, Middle and Inferior lakes are characterized by high turbidity and eutrophic conditions, and water level is kept fixed to prevent flowing the city of Mantua. Macrophyte communities in the system are populated by both autochthonous (*T. natans*, *N. lutea*, *N. alba* in open water areas, and *P. australis* in wetlands) and allochthonous species (Pinardi *et al.*, 2011; Villa *et al.*, 2017; Tóth *et al.*, 2019): *Nelumbo nucifera* Gaertn., introduced into the lake for different purposes around a century ago, and *Ludwigia hexapetala* (Hook. & Arn.) Zardini, H.Y. Gu & P.H. Raven, which started spreading here during the last decade.

Lake Varese, located in subalpine northern Italy (45°49′ N, 8°44′ E; 238 m a.s.l., is a monomictic, eutrophic lake (area: 14.2 km^2; average depth: 10.9 m) subject to high anthropic pressures and nutrient loads. The southern shores of the lake host extensive stands of floating macrophytes, mainly *T. natans* and *N. lutea*, with some presence of *N. alba*. (Villa *et al.*, 2015). Some tracts of littoral zone have been colonized in the last couple of decades by allochthonous species, *N. nucifera* and *L. hexapetala*.

2.2. Field measurements

Boat-based surveys were carried out in the three sites for three years (2016-2018), covering different times within the macrophyte growing season, spanning from late May to late July. Due to logistic and technical constraints, macrophyte beds sampled were not always the same ones in different years. During the surveys, leaf samples from 6 species showing sensitive presence in the study areas (*L. hexapetala, N. nucifera, N. alba, N. lutea. P. australis, T. natans*) were measured and collected over various locations, to incorporate intra-site variability. A summary of sampling locations for each species and survey date is provided in Supplementary Table 1. Leaf samples were collected from plants growing in dense (canopy fraction cover > 60%) and homogeneous stands, within 3 m of the water edge; from each plant sampled, the youngest, mature leaf directly exposed to sunlight was taken for measurements.

2.2.1.Leaf spectral reflectance

Leaf reflectance in the visible to shortwave infrared range (350 – 2500 nm, spectral resolution of 3 nm for wavelengths under 1000 nm, and < 8 nm up to 2500) was measured using a portable full range spectroradiometer (SR-3500, Spectral Evolution, Lawrence, USA), over the same leaves sampled for chlorophyll fluorescence measurements, following the protocol described in Tóth *et al.* (2019). After the 20-minute dark adaptation, leaves were de-shadowed and laid on a flat neoprene plate (reflectance factor < 5%) in order to minimize background reflection of light transmitted through the leaves. Leaf reflected radiance was measured at contact using a probe equipped with 5-watt internal light source under near-steady state conditions, i.e. 60 seconds after de-shadowing. Each spectrum is the result of 10 averaged scans, and automatic integration time optimization was used, with a maximum allowed of 50 ms per scan. Leaf spectra were finally calibrated to reflectance using reflected radiance from a Spectralon panel (Labsphere, North

Sutton, USA; reflectance factor > 99% for wavelengths under 1500 nm, and > 95% up to 2500 nm) as reference.

2.2.2.Leaf photophysiology

Photophysiological traits of macrophytes were assessed using chlorophyll fluorescence measured with a PAM-2500 chlorophyll fluorometer (Heinz Walz GmbH, Germany). Data were collected occasionally between 09:00 and 15:00, standard solar time. Relevant fluorescence yield data (initial fluorescence yield - F_0, maximal fluorescence yield - F_m) were measured following the protocol described in Tóth *et al.* (2019) on mature, healthy-looking leaves after a dark-adapting period of 20 minutes with a pulse of a saturated light (630 nm, intensity 3000 µmol m^{-2} s^{-1}). Photochemical PSII efficiency (F_v/F_m), coefficient of photochemical quenching (qP), coefficient of non-photochemical quenching (qN), maximum electron transport rate of the photosystem II (PSII) (ETR_{max}), theoretical saturation light intensity (I_k), and maximum quantum yield for whole chain electron transport (α) were calculated using fluorescence yield data and a light response curve - function of ETR to photosynthetically active radiation (PAR) in 11 steps between 5 and 787 µmol m^{-2} s^{-1} - described by an exponentially saturating equation (Eilers & Peeters, 1988; Genty *et al.*, 1989).

2.2.3.Leaf pigments and economics traits

Two leaf discs (0.6 cm in diameter) were cut with a cork borer from each fresh leaf, in the vicinity of where chlorophyll fluorescence was measured. Disks were stored in aluminium foil at sub 0 temperature in a camping fridge until they were transferred to the laboratory, i.e. within maximum 4 hours.

Half of the discs sampled were stored in -20° C freezer, to be used for pigments extraction, following the protocol described in Tóth *et al.* (2019). Upon extraction, they were homogenised in liquid N_2 in a grinder, subsequently extracted in acetone solution (80%), and stored in a fridge overnight. The extracts were centrifuged and the supernatant collected and stored at –20 °C. The full spectra of absorbance of the extracts were measured between 400 nm and 750 nm using a spectrophotometer (Shimadzu UV-2401PC, dual-beam), at 1 nm resolution. Finally, pigment concentrations, i.e. chlorophyll-a (Chl-a), chlorophyll-b (Chl-b), and total carotenoids (Car), were calculated using empirical formulae (Wellburn, 1994) and reported on leaf area basis (µg cm^{-2}). Pigments ratios were then calculated, as Chl-a to Chl-b ratio (Ca/Cb) and total chlorophylls (Chl-a + Chl-b) to total carotenoids ratio (Chl/Car).

The other half of leaf discs were weighted with a precision balance (Mettler Toledo AB104, 0.0001 g accuracy) to measure their fresh weight, and were then dried in ventilated oven at 70° C for 48h, after which the dry weight was measured using the same balance. From these data, dry matter content (DMC) and leaf mass per area (LMA) of each disc were calculated as the ratio of dry weight to fresh weight (g g^{-1}), and the ratio of dry weight to disc area (g m^{-2}) respectively.

2.3. Spectral indices and leaf traits

For each possible combination of two spectral reflectance bands measured as described in Section 2.2.2 within the range 400-2500 nm (987 bands), the normalized difference spectral index (NDSI) was calculated

using a custom-made R script (Stratoulias *et al.*, 2015). NDSI are frequently used in RS because they offer the advantage of summarizing spectra information, while reducing uncertainty due to sensor differences and atmospheric effects and bias due to differences in vegetation background (Glenn *et al.*, 2008; Ustin *et al.*, 2009), and are defined as:

$$NDSI_{i,j} = \frac{\rho_i - \rho_j}{\rho_i + \rho_j} \quad (1)$$

Where ρ is leaf reflectance measured at spectral bands i or j.

Using the same R script, the correlation (Pearson's r) between each leaf parameter, i.e. photophysiology, pigments and economics trait, and every calculated NDSIs was calculated together with the corresponding p-value (p). Correlation plots featuring the coefficient of determination (R^2), calculated as the square of r, between each leaf parameter and the complete combinations of NDSIs derived from leaf reflectance were drawn for significant relations ($p < 0.01$), in order to highlight optimal two-band combinations proxies of investigated leaf photophysiology (α, ETR_{max}, I_k, F_v/F_m, qN, qP), pigments pool (Chl-a, Chl-b, Car, Ca/Cb, Chl/Car), and leaf economics (DMC, LMA) traits.

2.4. Hyperspectral modelling of leaf traits

Partial least-square regression (PLSR) modelling (Geladi & Kowalski, 1986) was used to further explore the relations between leaf reflectance and selected leaf traits across floating and emergent macrophyte species, using package *pls 2.7*, implemented in R (Mevik & Wehrens, 2007; R Development Core Team, 2018). PLSR is a powerful tool for modelling vegetation parameters using spectral datasets, because it is suitable for cases when number of predictors is larger than that of observations and can handle multi-collinearity in predictor variables, as frequently happens with narrow-band hyperspectral data (Wold *et al.*, 2001; Feilhauer *et al.*, 2010).

In order to focus on meaningful relations, PLSR models were calibrated only for leaf traits that showed enough sensitivity to spectral reflectance, that is scoring a R^2 against all combinations of NDSIs higher than 0.15 (with $p < 0.01$), while excluding mutually correlated traits (i.e. scoring Pearson's r *vs.* any other trait < -0.5, or > 0.5). The number of PLSR components used for each calibrated model (with 30 components set as maximum) was optimized through minimization of the root mean square error of prediction (RMSEP). The best model for each trait was eventually selected by setting the number of PLSR components corresponding to minimum cross-validation RMSEP, and model performance was assessed via leave-one-out cross-validation, comparing measured with PLSR model predicted trait values.

2.5. Airborne hyperspectral images

Airborne hyperspectral images of Lake Hídvégi and Mantua lakes system were acquired from the APEX imaging spectrometer (Schaepman *et al.*, 2015) on 19 July 2014 (around 12:00 local time) and 27 September 2014 (around 13:45 local time), respectively. Visible to near-infrared range APEX data were processed,

resulting in hyperspectral images composed by 98 spectral bands (425-905 nm), with 3-10 nm spectral resolution.

APEX data were calibrated to at-sensor radiance units and georeferenced based on sensor's GPS/IMU at 5 m spatial resolution on the ground. Surface reflectance was finally derived by applying atmospheric correction based on MODTRAN-4 code and optimized for water targets (De Haan *et al.*, 1991).

To demonstrate the potential of hyperspectral remote sensing data in highlighting spatial patterns of macrophyte traits, maps of spectral proxies were derived from APEX surface reflectance bands by calculating the NDSI based on the optimal two-band combination for leaf traits whose NDSI-trait relation scored an $R^2 > 0.4$ within the spectral range covered by APEX bands.

3. Results

3.1. Variability of macrophyte leaf traits

Regarding traits related to photosynthetic performance, allochthonous species outperformed autochthonous ones, i.e. *Nelumbo* scored the highest α ($p = 0.002$, Kruskal-Wallis One Way ANOVA), and *Ludwigia* scored the highest ETR_{max}, I_k and qP ($p < 0.001$, Kruskal-Wallis One Way ANOVA). Moreover, regulated thermal dissipation of excess absorbed light (qN) was found being slightly lower in *Nelumbo* and *Ludwigia*, as well as in *Trapa*, compared to nymphaeids (*Nuphar* and *Nymphaea*) and *Phragmites* (Fig. 1; Supplementary Fig. S1). The only outstanding native species was *Phragmites*, as it showed quantum efficiency of photosystem II (F_v/F_m) slightly higher than all other species ($p < 0.001$, Kruskal-Wallis One Way ANOVA).

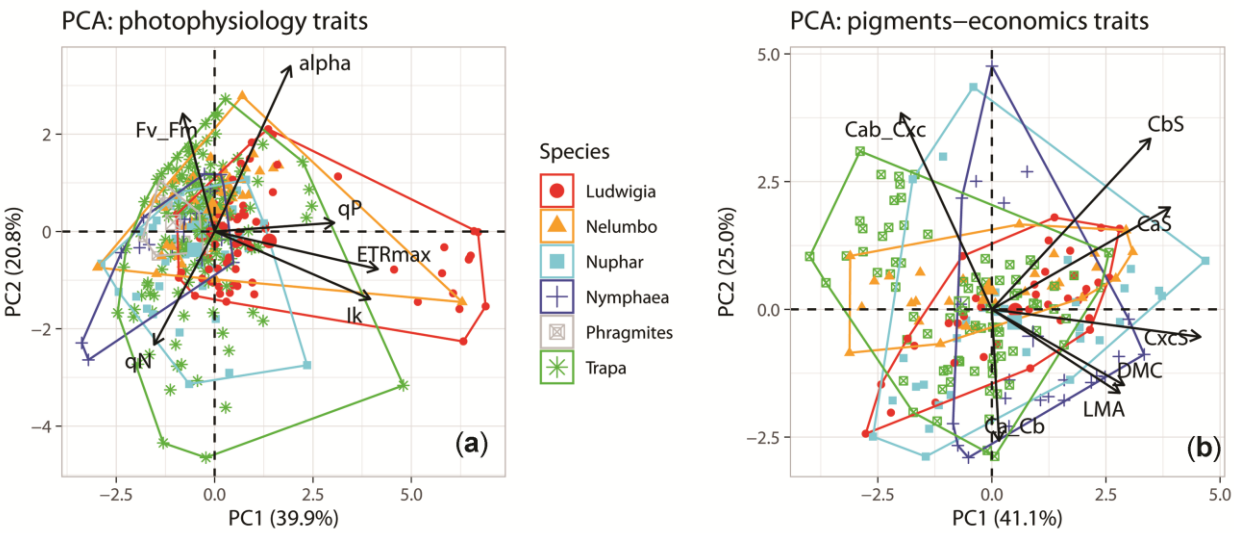

Figure 1. Bi-plots of the first two Principal Components of leaf photophysiological parameters (left panel) and pigments content and leaf economics spectrum traits (right panel), measured over all macrophyte species sampled. alpha - maximum quantum yield for whole chain electron transport; ETRmax - maximal electron transport rate; Ik - theoretical saturation light intensity; Fv_Fm - PSII photochemical efficiency; qP - coefficient of photochemical quenching; qN - coefficient of non-photochemical quenching; CaS – chlorophyll a content; CbS - chlorophyll b content; Cxc – total carotenoids content; Ca_Cb - chlorophyll a to chlorophyll b ratio; Cab_Cxc - chlorophylls to carotenoids ratio; DMC – leaf dry matter content; LMA - leaf mass per area.

Ludwigia and *Nelumbo* displayed Chl-a values slightly higher than autochthonous species ($p = 0.012$, Kruskal-Wallis One Way ANOVA), while no significant difference across species was observed for Chl-b, and highest carotenoid content was found in *Nelumbo* and *Trapa* ($p < 0.001$, Kruskal-Wallis One Way ANOVA). Nymphaeids got the lowest Ca/Cb ratio among species, with *Ludwigia* occupying the high band of scores ($p < 0.001$, Kruskal-Wallis One Way ANOVA). A strong level of segmentation at species level was shown for Chl/Car ratio ($p < 0.001$, Kruskal-Wallis One Way ANOVA): *Nelumbo* and *Trapa* exhibited the highest scores and *Ludwigia*, *Nuphar*, *Nymphaea* followed in decreasing Chl/Car.

Compared to autochthonous species, leaf DMC was higher ($p < 0.001$, Kruskal-Wallis One Way ANOVA) and LMA lower ($p < 0.001$, Kruskal-Wallis One Way ANOVA) for both *Ludwigia* and *Nelumbo* (Fig. 1; Supplementary Fig. S1). Inter-species DMC patterns tend to be similar to those of Chl/Car, with the exception of *Trapa*, and a strong differentiation in LMA was observed among species, with nymphaeids scoring the highest values and *Trapa* spanning the widest range (Fig. 1; Supplementary Fig. S1).

Table 1. Coefficient of variation (CV) of all leaf traits measured over macrophytes species sampled (highest scores across species for each trait are in bold, lowest in italic).

Species	**Photophysiology parameters**						**Leaf pigments**					**Leaf economics**	
	α	**ETR_{max}**	**I_k**	**F_v/F_m**	**qN**	**qP**	**Chl-a**	**Chl-b**	**Car**	**Ca/Cb**	**Chl/Car**	**DMC**	**LMA**
Ludwigia	0.135	**0.931**	**0.782**	0.058	**0.317**	*0.109*	0.287	0.273	*0.231*	0.101	0.111	0.150	*0.155*
Nelumbo	0.130	0.740	0.597	0.048	0.254	0.192	0.281	0.261	0.294	*0.088*	*0.092*	0.200	0.214
Nuphar	0.174	0.531	0.741	0.068	0.163	0.232	**0.312**	**0.362**	**0.340**	0.157	0.246	0.155	0.263
Nymphaea	**0.184**	0.355	0.227	0.050	0.168	**0.347**	*0.181*	0.339	0.286	**0.265**	**0.357**	*0.126*	0.198
Phragmites	*0.074*	*0.172*	*0.187*	*0.044*	*0.072*	0.156	-	-	-	-	-	-	-
Trapa	0.174	0.479	0.563	**0.098**	0.300	0.243	0.218	*0.212*	0.243	0.092	0.181	**0.319**	**0.395**

Leaf data collected exhibited a notable degree of intraspecific variability for most of the traits (Fig. 1), with maximum coefficient of variation (CV) across all species larger than 0.25 with the only exceptions of α and F_v/F_m (Table 1). *Phragmites* presented the lowest variable set of photophysiology traits except for qP (CV < 0.19), while nymphaeids had the most variable traits (α, qP, Ca/Cb and Chl/Car for *Nymphaea*; Chl-a, Chl-b and Car for *Nuphar*). *Ludwigia* showed very high plasticity in photophysiology parameters ETR_{max}, I_k, and qN (CV > 0.31), and *Trapa* scored highest intraspecific ranges of DMC and LMA (CV > 0.31).

3.2. Spectral indices as proxies for macrophyte leaf traits

The correlations of every two-band combination NDSI correlations with all the investigated leaf traits parameters measured on all macrophyte species sampled are highlighted in Fig. 2-4, showing the optimal spectral proxies for each trait in the visible to near-infrared (VNIR) spectral range (400-1000 nm) and in full spectral range (400-2500 nm), i.e. extending to shortwave infrared (SWIR) wavelengths.

The heterogeneity of measured samples not only in terms of species, but also in terms of location (three study sites) and time of sampling (three years, different months) - which implies that our dataset includes a high variability in genetic features, seasonal cycles, stage of growths, condition and environmental

circumstance - overall resulted in relatively low correlation patterns ($R^2 < 0.26$) between leaf reflectance derived NDSI and measured photophysiological traits (Figure 2). In particular, negligible (even if $p < 0.01$) correlations with any NDSI combinations were shown across all species for α, ETR_{max}, I_k, qN (overall maximum $R^2 = 0.10$). Slightly higher but still moderately weak correlations are shown for F_v/F_m and qP, with R^2 peaking at 0.19 and 0.25, respectively (Fig. 2). The optimal NDSI for F_v/F_m combined reflectance in the range of green visible light (524 nm, 581 nm), while for qP the best spectral combinations lied in the SWIR range, roughly around 1400-1500 nm.

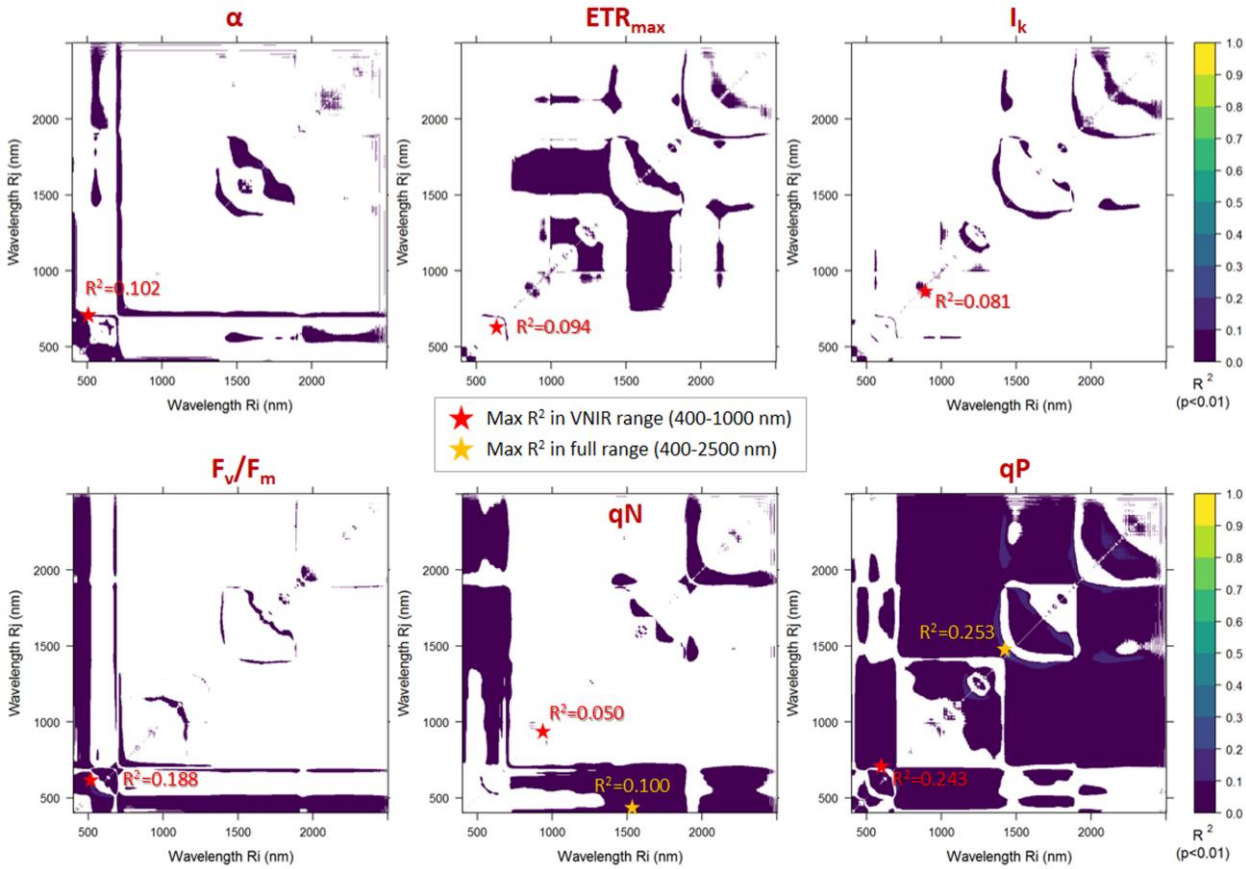

Figure 2. Statistically significant ($p < 0.01$) NDSI correlations with photophysiological parameters measured on all macrophyte species sampled (N=324).

Regarding pigments content and ratios, the heterogeneity mentioned above as biasing the reflectance-photophysiology relations did not bring to low correlations with leaf reflectance NDSI across species, as peak R^2 found was always higher than 0.3 (Fig. 3). In particular, good correlation between NDSIs and Chl-a were found, particularly in the red-edge range (maximum $R^2 = 0.43$ for $NDSI_{775,740}$). As Chl-b is highly correlated with Chl-a in our dataset ($r = +0.80$), optimal band combinations are found around the same range highlighted for Chl-a (795 nm, 740 nm), yet with slightly weaker correlation (maximum $R^2 = 0.37$). Among pigments, Car showed the strongest correlations, peaking at NDSIs featuring band combinations in the SWIR range (maximum $R^2 = 0.57$ for $NDSI_{1644,1720}$), while correlations decreased if spectral range was limited to VNIR (maximum $R^2 = 0.37$). Ca/Cb ratio showed the weakest correlations of all pigment traits, with a peak

$R^2 = 0.31$ in the SWIR range (for $NDSI_{2181,2241}$). Chl/Car ratio is instead very well surrogated by NDSIs combining visible to SWIR reflectance (maximum $R^2 = 0.60$ for $NDSI_{611,1892}$); slightly lower correlations, yet still the highest among all pigments traits measured (maximum $R^2 = 0.55$), were scored restricting the spectral range to VNIR range, where optimal NDSI for Chl/Car combined reflectance in 433 nm and 665 nm, that indeed roughly correspond to absorption peaks of chlorophyll-a (Ustin *et al.*, 2009).

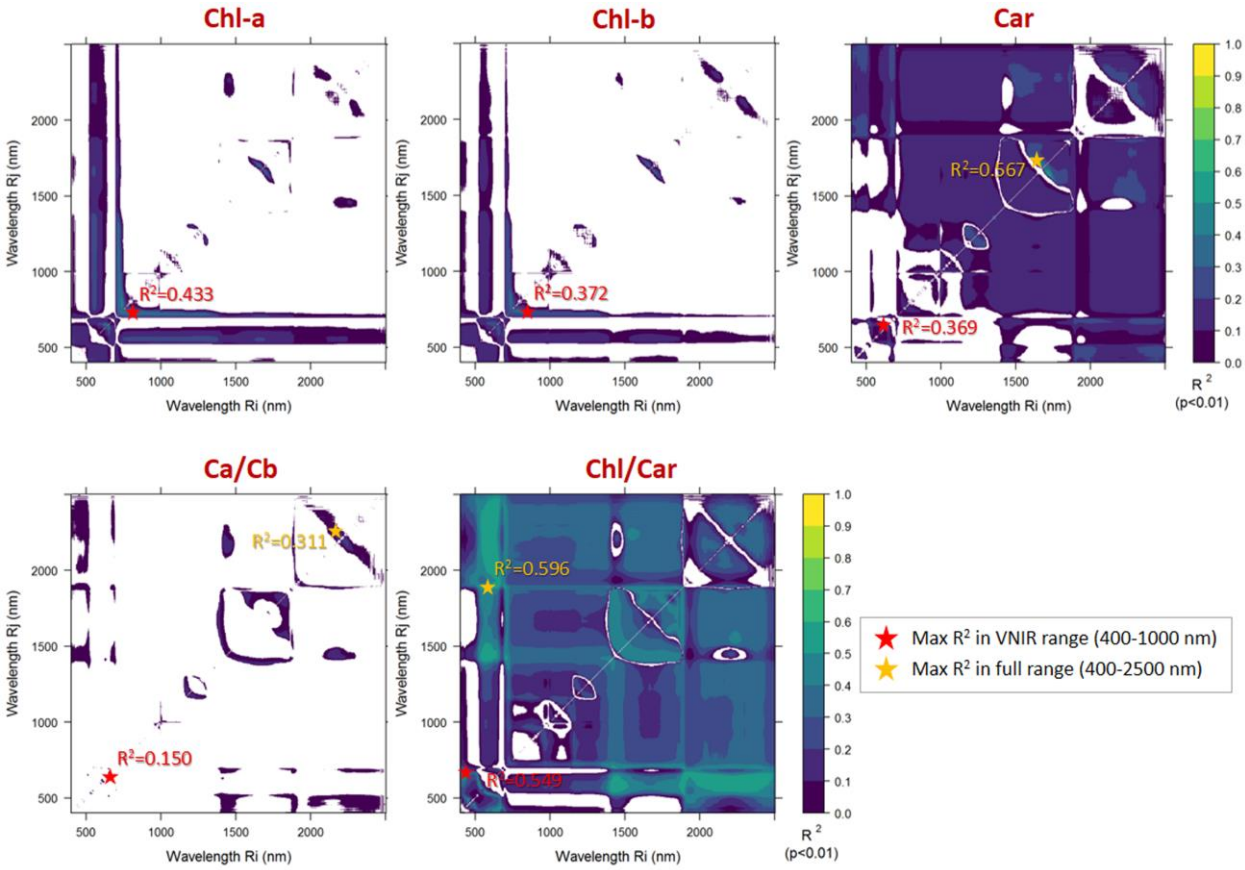

Figure 3. Statistically significant ($p < 0.01$) NDSI correlations with pigments content (on leaf area basis) and their balance measured on all macrophyte species sampled (N=150).

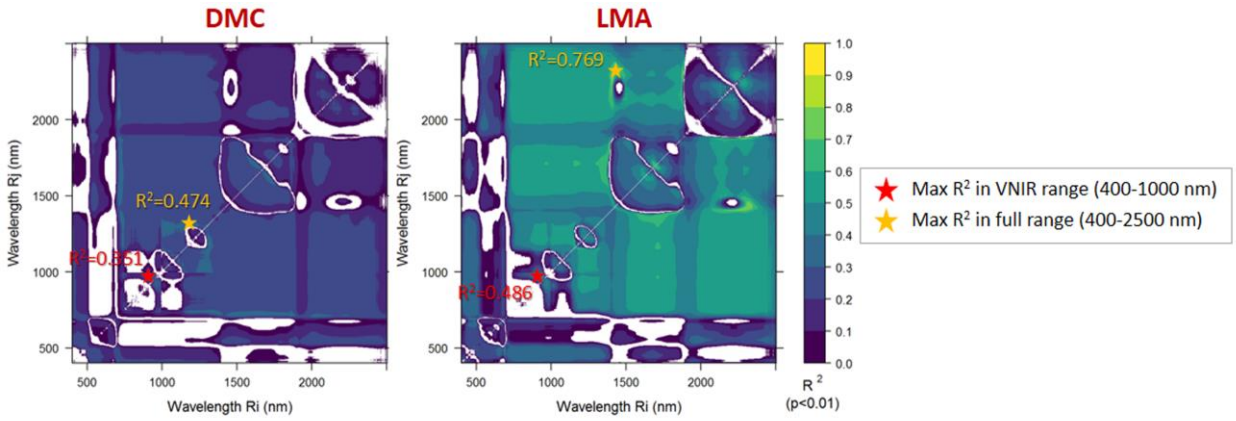

Figure 4. Statistically significant ($p < 0.01$) NDSI correlations with leaf economics traits, measured on all macrophyte species sampled (N=152): leaf dry matter content (DMC) and leaf mass per area (LMA).

Strong correlations were scored between NDSI derived and leaf structural traits measured, DMC and LMA (Fig. 4), connected to leaf economics. DMC demonstrated a good sensitivity to leaf reflectance in the NIR to SWIR ranges, with R^2 up to 0.47 for $NDSI_{1196,1308}$, with slightly weaker scores in the shorter wavelengths (maximum $R^2 = 0.35$ for $NDSI_{929,941}$). Among all leaf traits, LMA scored the highest correlations with NDISs, with a large subset of band combinations showing $R^2 > 0.6$ in the NIR to SWIR ranges, and a peak $R^2 = 0.77$ when two bands at 1415 and 2305 nm were used (Fig. 4).

3.3. Leaf reflectance-traits relations

After having assessed mutual correlations of measured leaf traits, excluding the ones with $|r| > 0.5$, PLSR models were calibrated for traits scoring non negligible correlations with best performing NDSI presented in previous section ($R^2 > 0.15$): F_v/F_m, qP, Chl-a, Ca/Cb, Chl/Car, DMC, LMA (Fig. 5).

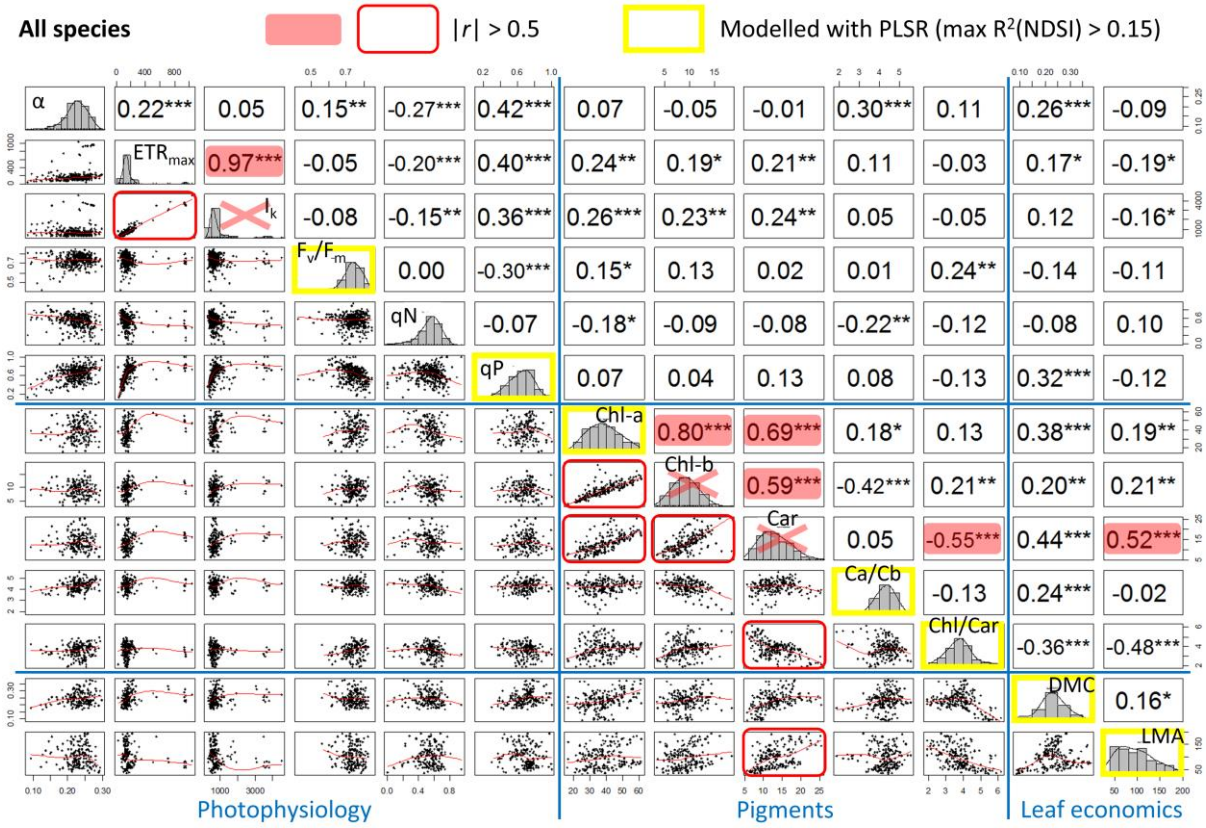

Figure 5. Correlation matrix of leaf traits measured over 6 species. Pair-wise scatter plots are shown in the lower left half, histograms are shown on the diagonal, and the coefficient of correlation (Pearson's *r*) of each pair of traits is shown in the upper right half, including info about its significance level (* p<0.05, ** p<0.01, *** p<0.001).

The best fit PLSR models for F_v/F_m and qP require 11 components, with RMSEP of 0.053 and 0.125 respectively (Fig. 6). Matching between measured and predicted photophysiology traits was slightly higher, $R^2 = 0.21$ for F_v/F_m and $R^2 = 0.33$ for qP, than what found for best performing spectral indices ($R^2 = 0.19$ and 0.25, respectively). These performance holds across the whole range of measures in our dataset (N = 324), but estimation error seem to be reducing when extreme values - probably due to stress conditions non visibly

detected when leaves were chosen for sampling – are excluded, i.e. for $F_v/F_m > 0.65$ and for $0.4 < qP < 0.8$ (Fig. 7).

PLSR models based on leaf reflectance are effective in predicting macrophyte Chl-a content (on area basis) and Chl/Car ratio across species, with best fit models requiring 11 and 13 components respectively (RMSEP of 7.52 µg cm^{-2} and 0.393; Fig. 6). Across the whole range of measures in our dataset (N = 150-151) the matching between measured and predicted pigments is slightly higher - $R^2 = 0.46$ for Chl-a, and $R^2 = 0.65$ for Chl/Car (Fig. 7) - than what found for best performing spectral indices, respectively by 0.03 and 0.05. Conversely, modelling performance for Ca/Cb is moderately low ($R^2 = 0.20$), sensibly lower than best performing NDSI ($R^2 = 0.31$), suggesting that spectral reflectance might not be a good proxy for this trait, at least for macrophyte species.

DMC and LMA are the leaf traits better surrogated by reflectance based models, with matching between measured and PLSR predicted scores up to RMSEP = 0.026 g g^{-1} (i.e. 2.6% leaf weight) for DMC ($R^2 = 0.68$ with 15 components, Fig. 6-7) and up to RMSEP = 18.6 g m^{-2} for LMA ($R^2 = 0.76$ with 11 components, Fig. 6-7), across the whole range of measures in our dataset (N = 152-153). PLSR outcomes are similar to what found for best performing spectral index for LMA ($R^2 = 0.77$ for $NDSI_{1415,2305}$), while they are sensibly better for DMC ($R^2 = 0.47$ with $NDSI_{1196,1308}$).

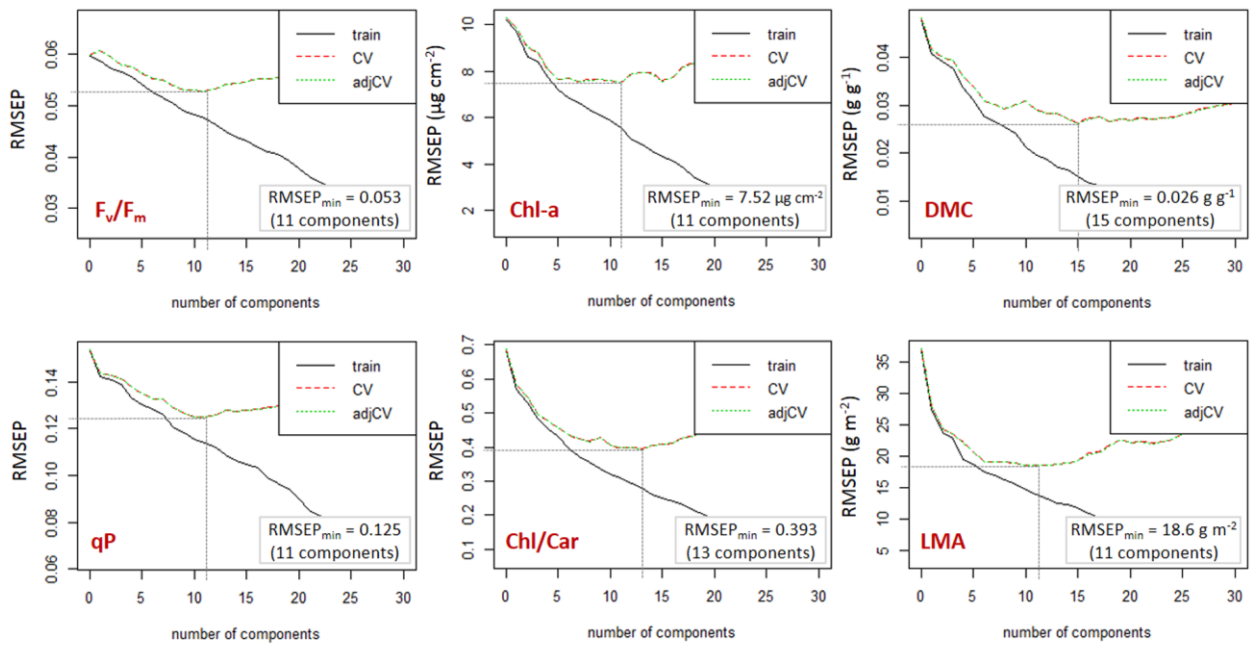

Figure 6. Variation of root mean square error of prediction (RMSEP) with PLSR model components, computed against the full dataset (training as well as via leave-one-out cross-validation (CV) for key leaf traits modelled based on leaf spectral reflectance of measured macrophyte species.

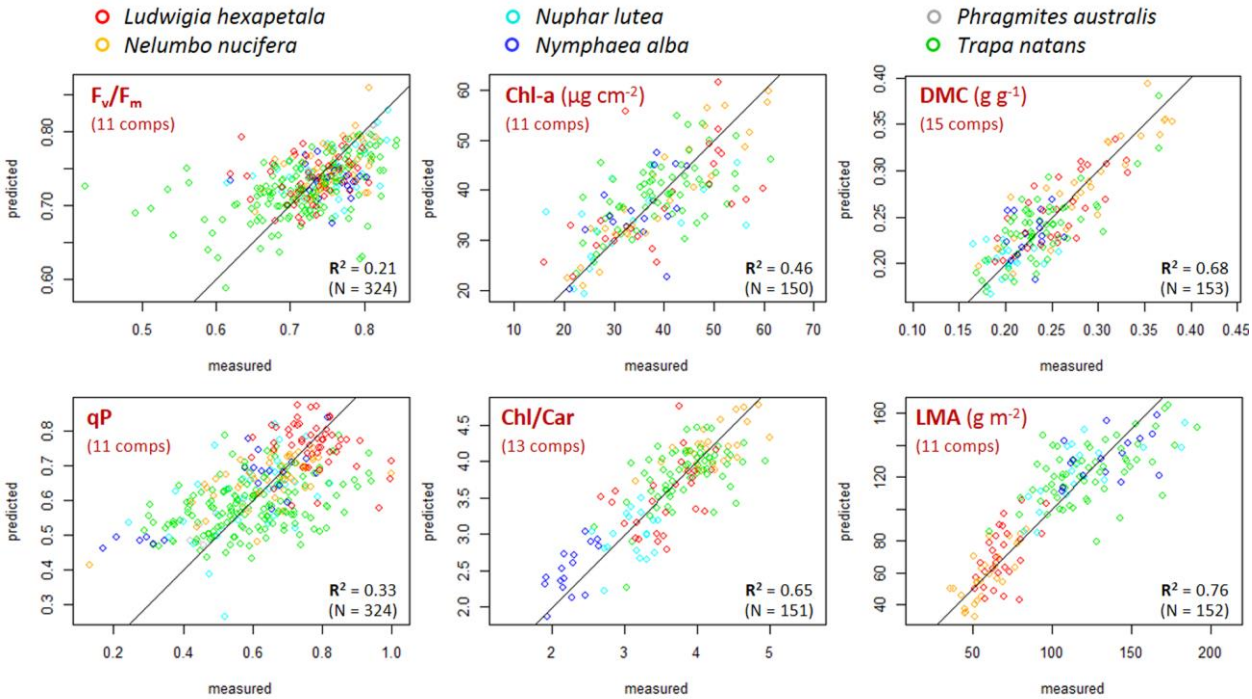

Figure 7. Comparison of leaf traits measured and predicted by best fit PLSR models for key leaf traits of selected macrophyte species, computed via leave-one-out cross-validation.

3.4. Mapping macrophyte traits from airborne hyperspectral images

The potential for application of the main findings described in previous sections was demonstrated by producing spatial variability maps of selected macrophyte traits by calculating specific NDSIs highlighted in section 3.2 based on airborne hyperspectral data, collected over Lake Hídvégi and Mantua lakes system from APEX during different times in the summer of 2014. Considering the spectral range of APEX data (425-905 nm), macrophyte traits spatial variability maps are derived only for those spectral indices showing best matching with *in situ* measured data: i.e. $NDSI_{775,740}$ as proxy of Chl-a content (R^2 = 0.43), $NDSI_{433,665}$ as proxy of Chl/Car ratio (R^2 = 0.55), and $NDSI_{690,500}$ as proxy of LMA (R^2 = 0.44).

We fully recognise that the application of NDSI proxies using RS data inevitably bring to more or less significant biases, reflecting into the reliability of plant functional traits retrieved, which are due to complex combinations of factors, including: vegetation fractional cover and mixture with canopy background, density and structure effects (e.g. leaf orientation), reflectance anisotropy, and atmospheric effects (Asner *et al.*, 2015). All the more so, spectral data measured from APEX airborne imager, with pixel size in this case of 5 m, are inherently measuring macrophyte beds responses at canopy scale, and application of proxies derived and assessed at leaf scale to some extent hampers the absolute matching of observation scales for spectral reflectance and plant traits.

Notwithstanding the above mentioned factors of distortion, APEX based maps of selected traits in Lake Hídvégi and Mantua lakes system, shown in Fig. 8, are clearly capturing notable patterns of relative

variability in macrophyte communities at within-system scale that are informative about specific features of macrophytes growing the two sites.

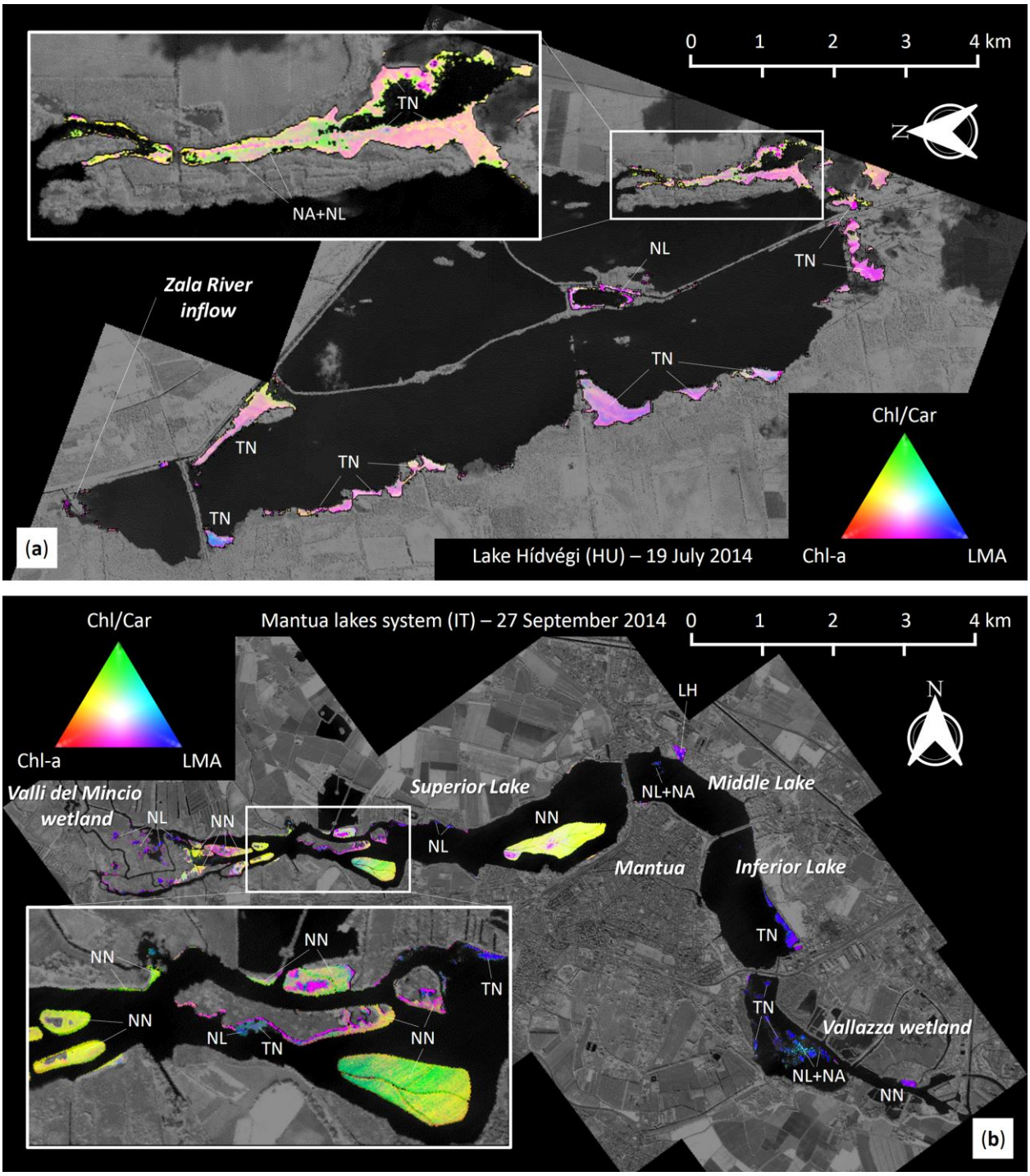

Figure 8. Maps of macrophyte trait spectral proxies derived from airborne hyperspectral (APEX) data over Lake Hídvégi (a) and Mantua lakes system (b), showing RGB combinations of best spectral proxies in the range covered by APEX data for: Chl-a content ($NDSI_{740,775}$), Chl/Car ratio ($NDSI_{433,665}$), and LMA ($NDSI_{690,500}$). LH: *Ludwigia hexapetala*; NN: *Nelumbo nucifera*; NL: *Nuphar lutea*; NA: *Nymphaea alba*; TA: *Trapa natans*.

Indeed, spatial patterns of variability in spectral proxies for three traits connected with the LES are highlighted within each site, showing differences at site scale, due to both inter- and intra-species differentiation (e.g. *Trapa* in Lake Inferior, *Nelumbo* in Lake Superior within Mantua lakes system, Fig. 8b),

as well as considerable variability at community scale, highlighting intra-specific trait plasticity (e.g. *Trapa* in Lake Hídvégi, Fig. 8a, and *Nelumbo* in Mantua lakes system, Fig. 8b). Moreover, differences in spatial patterns and ranges of trait proxies between and across the sites are due to species composition but also to seasonal differences, another factor that can be taken under control by using remote spectroscopy data, once relations with plant traits are established. In fact, APEX data collected over Lake Hídvégi in middle of July represent macrophyte conditions at peak of growth, while data for Mantua lakes system, acquired in late September, provide a static image of macrophyte communities in early to late senescence phase, depending on species.

4. Discussion

For the specific characteristics of their habitat, macrophytes can tolerate significant changes in environmental conditions during the growing season and across years, which may lead to alterations in physiological performance and community composition (Søndergaard *et al.*, 2010). Macrophyte leaf trait data collected – covering different sites (three shallow lakes and wetland in Europe), times (late May to late July), and seasons (three years) – showed a high degree of heterogeneity, both within and among species sampled (Fig. 1). Allochthonous, invasive species tended to achieve better photosynthetic performance compared to autochthonous ones (Van Kleunen et al., 2010; Tóth *et al.*, 2019), with *Nelumbo* showing the highest α (0.238±0.031 electrons/quanta), while *Ludwigia* surpassed other species in terms of ETR_{max} (306.7±285.7 µmol electrons m^{-2} s^{-1}), I_k (1358.1±1058.2 µmol quanta m^{-2} s^{-1}) and qP (0.771±0.085). Among native species, *Phragmites*, outperformed all others in terms of F_v/F_m (0.784±0.035), but as this came out of a small sample (N = 12), not including seasonal or site variability (Supplementary Table S1), the result needs to be ascertained with further data collection. In parallel with what observed for photophysiology, leaf economics traits of allochthonous species were found significantly different from those of other species, i.e. *Ludwigia* and *Nelumbo* have higher leaf DMC (0.264±0.040 and 0.290±0.059 g g^{-1}, respectively) and lower LMA (70.47±11.03 and 59.81±12.90 g m^{-2}, respectively), compared to autochthonous species (see Supplementary Fig. S1). Differently from what found on mass basis in previous works (Tóth *et al.*, 2019), foliar pigment content on area basis did not separate alien and native plants as distinctively as the photophysiological and leaf economic traits (Fig. 1). Instead, a certain degree of segmentation at species level was found for pigments balance measures, especially Chl/Car, thus suggesting that interspecific differentiation in aquatic plants could be driven more by secondary pigments than by chlorophyll-a, and therefore by the ability of species to balance light use maximization with need for photoprotection (Grimshaw *et al.*, 2002; Hussner *et al.*, 2010).

Substantive intraspecific variability in our empirical dataset was found, especially for photophysiological traits (ETR_{max} and I_k), with CV up to 0.93 for *Ludwigia*, strengthening what already observed over Mantua lakes system by Tóth *et al.* (2019). Nymphaeids showed the highest variability in pigments content (CV > 0.31 for *Nuphar*) and balance (CV > 0.26 for *Nymphaea*), while leaf economics traits for *Trapa* were the

most variable, also due to its spread all over the study sites and the highest number leaf samples out of measured species. Different species vary considerably in the lifespan of their leaves, resulting in increased foliar phenotypic plasticity (Wu *et al*., 2017), thus making direct functional interspecific comparison challenging, in connection with environmental factors (Kunii & Aramaki, 1992). Actual leaf age should therefore be taken into account for a thorough assessment of foliar trait variability among species, and it will be probably one of key topics in future works.

Leaf reflectance is affected by multiple characteristics, with tri-dimensional leaf structure being the dominant factor, as outer (e.g. trichomes, cuticle surface) and inner (e.g. amount and ratio of different mesophylls) elements are responsible for major scattering mechanisms (Sims & Gamon, 2002; Levizou *et al.*, 2004; Klančnik & Gaberščik, 2016). Light absorption as well can be dependent on leaf structural arrangements, as more chlorophyll molecules are usually found in the palisade parenchyma, i.e. closer to the adaxial surface of the leaves (Terashima & Hikosaka, 1995; Smith *et al.*, 1997), particularly when high porosity - the so-called aerenchyma in aquatic plants – is found (Borsuk & Brodersen, 2019).

Our key finding is that a suite of leaf functional traits, well connected with light absorption and scattering mechanisms, can be effectively modelled across macrophyte species based on leaf reflectance, even under moderate to strong environmental heterogeneity.

Best results were obtained via PLSR models for structural traits, i.e. leaf DMC (RMSEP = 0.026 g g^{-1}, or 10% in relative terms), and LMA (RMSEP = 18.6 g m^{-2}, or 18% in relative terms), which constitute synthetic descriptors of leaf morphology, and in particular the inner structure, mediating the effects of scattering mechanisms with water absorption. Indeed, maximum sensitivity of leaf reflectance to DMC was found in NIR (R^2 = 0.35) and SWIR ranges (R^2 = 0.47) for spectral indices combining bands located around the shoulder of water absorption features (Kokaly *et al.*, 2009). Leaf reflectance-LMA connections revealed a more complex picture, with optimal spectral ranges found for macrophyte species sampled (R^2 up to 0.77, for $NDSI_{1415,2305}$) that confirmed what documented from previous works on terrestrial plants about correlations between leaf reflectance and LMA at macro spectral ranges, i.e. in the SWIR (le Maire *et al.*, 2008; Féret *et al.*, 2011; Wang & Li, 2012; Ali *et al.*, 2017; Féret et al:, 2019), but with specific differences in optimal wavelengths to be used, possibly because of peculiarities in leaf structure of macrophytes, compared to terrestrial plants (Klančnik & Gaberščik, 2016).

The other traits showing good PLSR modelling performance across species - i.e. Chl-a content (RMSEP = 7.52 µg cm^{-2}, or 19% in relative terms) and Chl/Car ratio (RMSEP = 0.393, or 11% in relative terms) - were dealing with leaf pigments pool, which can be mainly located in the first adaxial strata of floating aquatic plant leaves, as shown for chlorophylls in the case of *Eichornia crassipes* (Mart.) Solms by Borsuk & Brodersen (2019). Consistently, weak correlations scored for Chl-b (R^2 = 0.37) could be explained by higher relative importance of Chl-b near the abaxial side, as Ca/Cb ratio is gradually decreasing with light penetration into the leaf (Terashima & Hikosaka, 1995). In general, relations found between leaf reflectance and pigments (Fig. 3), confirm and strengthen the notion that leaf spectral reflectance in the visible to NIR

range, commonly used for RS of vegetation properties, can be used as effective proxy for leaf pigments (and biochemistry) in macrophytes. Optimal spectral indices for Chl-a were found in the red-edge range (i.e. around 700-800 nm), similar to what extensively documented for terrestrial plants (Gitelson *et al.*, 2003; le Maire *et al.*, 2008; Féret *et al.*, 2011; Wang & Li, 2012). High NDSI-pigments correlations outside of PAR range, where pigments absorption is virtually null, can be attributed to interactions with other leaf traits (Fig. 5), i.e. correlation with LMA for Car (r = +0.52) and Chl/Car (r = -0.48). Instead, best performing spectral combinations for Ca/Cb ratio found around 2200 nm is possibly linked to N content (which we did not measure), that can be related to Ca/Cb (Kitajima & Hogan, 2003) and for which absorption features around 2180 nm were found in previous works (Kokaly, 2001; Li *et al.*, 2018).

The similarity between chlorophyll-a fluorescence dynamics and growth data suggests a close mechanistic link between photophysiological features and actual metabolism of plants (Genty *et al.* 1989; Peterson *et al.*, 2001). In presence of high spatial structuring, populations can exhibit large phenotypic plasticity (Santamaría, 2002; Bornette & Puijalon, 2011), in the form of either trait variability patterns within monospecific populations or specific trait distributions within mixed communities (Loreau & Hector, 2001), that can change with time (Thomaz *et al.*, 2009). Compared to what highlighted for leaf economics (structural) and pigments traits, reflectance-based PLSR models for photophysiological parameters were found to be under-performing across the species sampled: best results were scored for F_v/F_m (RMSEP = 0.053, or 7% in relative terms), with optimal spectral range very similar to photochemical reflectance index (PRI) linked to light use efficiency and xanthophyll cycle (Harris *et al.*, 2014), and qP (RMSEP = 0.125, or 20% in relative terms), whose best spectral proxies were found in the SWIR range, roughly around 1400-1500 nm, probably due to co-variation of qP with DMC (r = +0.32, Fig. 5). Sensitivity of chlorophyll fluorescence measures even to moderately small environmental variations, paired with the large spatial-temporal variability typical of macrophyte populations and represented into our empirical dataset (Fig. 1; Table 1; Supplementary Table S1) could constitute a relevant obstacle to the establishment of general reflectance-photophysiology traits models, requiring specific spectral models limited to species and/or phenological stage scales (Supplementary Fig. S3-S7), as done by Stratoulias & Tóth (2020) for *Phragmites*.

Our results demonstrate that spectral reflectance can be used for reliably estimating specific macrophyte leaf traits, i.e. Chl-a, Chl/Car, DMC and LMA, which are strongly connected to variability expressed within the LES in terms of trade-off between structural investment and photosynthetic efficiency (Poorter *et al.*, 2009; Onoda *et al.*, 2017; Ji *et al.*, 2020), by using normalized spectral indices or PLSR modelling based on an empirical dataset collected across sites, seasons, and species. This finding provide the basis for using leaf spectra as a surrogate for high-throughput assessment of macrophyte community functional diversity over scales and gradients, and support the extension of the reflectance-based trait modelling to RS spectroscopic data for enhancing the level of detail of functional diversity analysis, taking into full account fine-scale variability in plant function.

The possibility of using spectral proxies for modelling LMA, a key trait in the LES, at large scale and under spatial and temporal gradients, based on the strong links found with macrophyte leaf reflectance, similarly to what recently demonstrated for tropical forest species (Serbin *et al.*, 2019), opens intriguing perspectives for future research and applications to macrophyte diversity and functioning, as well as for plant science in general.

Spatial-wise maps of macrophyte traits, as the ones shown in Fig. 8, can provide intuitive, realistic and detailed *bio-visualisation* of vegetation diversity and connected processes. The extent and range of heterogeneity highlighted in Fig. 8 for macrophyte communities of Mantua lakes system and Lake Hídvégi could be hardly seen with punctual measurements of macrophyte traits, and yet it is captured in systematic, synoptic and quantitative way by applying leaf reflectance-traits relations we found to remotely sensed imaging spectroscopy data, informing us on spatial and temporal functional variability at inter- and intra-species level. Although some interesting case studies in this respect have been recently documented (e.g. Bolpagni *et al*., 2014; Tóth, 2018; Villa *et al.*, 2018), they were limited to one or few systems and few aquatic vegetation characteristics (functional types, phenology metrics), and wider, comprehensive applications on RS of macrophyte functional ecology can be advocated as further development of the approach here presented, possibly refining it for targeting more precisely how vegetation function is changing across plant communities in wetlands.

Remote sensing spectroscopy can allow the quantitative assessment of multiple comparisons between communities - at inter- and intra-specific levels, across spatial and temporal scales - and this work provides the basis for developing research applied to inland water systems and connected ecotones, almost neglected in functional studies largely biased toward terrestrial ecosystems (Gustafsson & Norkko, 2017), tackling hot environmental issues such as dynamics of aquatic ecosystem under climate change and anthropogenic influence, as well as mechanisms of invasions by alien species.

Author contributions

PV, VRT designed the study, collected the data, performed the analysis, and drafted the manuscript. RB, MP supported collection of data and interpretation of results. All authors reviewed and edited the final manuscript.

Acknowledgements

The authors thank the Parco del Mincio authority and voluntary ecological guards for support given during fieldwork on the Mantua lakes system.

This work was supported under the agreement on scientific cooperation between the Hungarian Academy of Sciences and the Consiglio Nazionale delle Ricerche (MacroSense project), and by the Hungarian National

Research, Development and Innovation Office, NKFIH [Grant No. KH-129505]. Part of the work was carried out in the context of the EU FP7 programme through the INFORM project [Grant No. 730066].

References

Abelleira Martínez OJ, Fremier AK, Günter S, Ramos Bendaña Z, Vierling L, Galbraith SM, Bosque-Pérez NA, Ordoñez JC. 2016. Scaling up functional traits for ecosystem services with remote sensing: concepts and methods. *Ecology and Evolution* 6: 4359–4371.

Albert CH, de Bello F, Boulangeat I, Pellet G, Lavorel S, Thuiller W. 2012. On the importance of intraspecific variability for the quantification of functional diversity. *Oikos* 121: 116–126.

Ali AM, Darvishzadeh R, Skidmore AK, van Duren I. 2017. Specific leaf area estimation from leaf and canopy reflectance through optimization and validation of vegetation indices. *Agricultural and Forest Meteorology* 236: 162–174.

Asner G, Martin R. 2008. Spectral and chemical analysis of tropical forests: Scaling from leaf to canopy levels. *Remote Sensing of Environment* 112: 3958–3970.

Asner GP, Martin RE, Carranza-Jiménez L, Sinca F, Tupayachi R, Anderson CB, Martinez P. 2014. Functional and biological diversity of foliar spectra in tree canopies throughout the Andes to Amazon region. *New Phytologist* 204: 127–139.

Asner GP, Martin RE, Anderson CB, Knapp DE. 2015. Quantifying forest canopy traits: Imaging spectroscopy versus field survey. *Remote Sensing of Environment* 158: 15–27.

Bolpagni R, Bresciani M, Laini A, Pinardi M, Matta E, Ampe EM, Giardino C, Viaroli P, Bartoli M. 2014. Remote sensing of phytoplankton-macrophyte coexistence in shallow hypereutrophic fluvial lakes. *Hydrobiologia* 737: 67–76.

Bornette G, Puijalon S. 2011. Response of aquatic plants to abiotic factors: a review. *Aquatic Sciences* 73: 1–14.

Borsuk AM, Brodersen CR. 2019. The Spatial Distribution of Chlorophyll in Leaves. *Plant Physiology* 180: 1406–1417.

Bridgham SD, Megonigal JP, Keller JK, Bliss NB, Trettin C. 2006. The carbon balance of North American wetlands. *Wetlands* 26: 889–916.

Butler EE, Datta A, Flores-Moreno H, Chen M, Wythers KR, Fazayeli F, Banerjee A, Atkin OK, Kattge J, Amiaud B, *et al.* 2017. Mapping local and global variability in plant trait distributions. *Proceedings of the National Academy of Sciences* 114: E10937–E10946.

Chuine I. 2010. Why does phenology drive species distribution? *Philosophical Transactions of the Royal Society B: Biological Sciences* 365: 3149–3160.

De Kroon H, Huber H, Stuefer JF, Van Groenendael JM. 2005. A modular concept of phenotypic plasticity in plants: Research review. *New Phytologist* 166: 73–82.

Dinka M, Ágoston-Szabó E, Urbanc-Berčič O, Germ M, Šraj-Kržič N, Gaberščik A. 2008. Reed Stand Conditions at Selected Wetlands in Slovenia and Hungary. In: Vymazal J, eds. *Wastewater Treatment, Plant Dynamics and Management in Constructed and Natural Wetlands*. Springer, Dordrecht, 1-12.

Elzinga JA, Atlan A, Biere A, Gigord L, Weis AE, Bernasconi G. 2007. Time after time: flowering phenology and biotic interactions. *Trends in Ecology & Evolution* 22: 432–439.

Feilhauer H, Asner GP, Martin RE, Schmidtlein S. 2010. Brightness-normalized Partial Least Squares Regression for hyperspectral data. *Journal of Quantitative Spectroscopy and Radiative Transfer* 111: 1947–1957.

Féret J-B, François C, Gitelson A, Asner GP, Barry KM, Panigada C, Richardson AD, Jacquemoud S. 2011. Optimizing spectral indices and chemometric analysis of leaf chemical properties using radiative transfer modeling. *Remote Sensing of Environment* 115: 2742–2750.

Féret J-B, le Maire G, Jay S, Berveiller D, Bendoula R, Hmimina G, Cheraiet A, Oliveira JC, Ponzoni FJ, Solanki T, *et al.* 2019. Estimating leaf mass per area and equivalent water thickness based on leaf optical properties: Potential and limitations of physical modeling and machine learning. *Remote Sensing of Environment* 231: 110959.

Franklin P, Dunbar M, Whitehead P. 2008. Flow controls on lowland river macrophytes: A review. *Science of The Total Environment* 400: 369–378.

Gamon JA, Somers B, Malenovský Z, Middleton EM, Rascher U, Schaepman ME. 2019. Assessing Vegetation Function with Imaging Spectroscopy. *Surveys in Geophysics* 40: 489–513.

Geladi P, Kowalski BR. 1986. Partial least-squares regression: a tutorial. *Analytica Chimica Acta* 185: 1–17.

Genty B, Briantais J-M, Baker NR. 1989. The relationship between the quantum yield of photosynthetic electron transport and quenching of chlorophyll fluorescence. *Biochimica et Biophysica Acta (BBA) - General Subjects* 990: 87–92.

Gitelson AA, Gritz † Y, Merzlyak MN. 2003. Relationships between leaf chlorophyll content and spectral reflectance and algorithms for non-destructive chlorophyll assessment in higher plant leaves. *Journal of Plant Physiology* 160: 271–282.

Glenn E, Huete A, Nagler P, Nelson S. 2008. Relationship Between Remotely-sensed Vegetation Indices, Canopy Attributes and Plant Physiological Processes: What Vegetation Indices Can and Cannot Tell Us About the Landscape. *Sensors* 8: 2136–2160.

Grimshaw HJ, Havens K, Sharfstein B, Steinman A, Anson D, East T, Maki RP, Rodusky A, Jin K-R. 2002. The effects of shading on morphometric and meristic characteristics of Wild Celery, Vallisneria americana MICHX., transplants from Lake Okeechobee, Florida. *Fundamental and Applied Limnology* 155: 65–81.

Gustafsson C, Norkko A. 2019. Quantifying the importance of functional traits for primary production in aquatic plant communities (A Austin, Ed.). *Journal of Ecology* 107: 154–166.

de Haan JF, Hovenier JW, Kokke JMM, van Stokkom HTC. 1991. Removal of atmospheric influences on satellite-borne imagery: A radiative transfer approach. *Remote Sensing of Environment* 37: 1–21.

Harris A, Gamon JA, Pastorello GZ, Wong CYS. 2014. Retrieval of the photochemical reflectance index for assessing xanthophyll cycle activity: a comparison of near-surface optical sensors. *Biogeosciences* 11: 6277–6292.

Homolová L, Malenovský Z, Clevers JGPW, García-Santos G, Schaepman ME. 2013. Review of optical-based remote sensing for plant trait mapping. *Ecological Complexity* 15: 1–16.

Hu Y-K, Pan X, Liu G-F, Li W-B, Dai W-H, Tang S-L, Zhang Y-L, Xiao T, Chen L-Y, Xiong W, *et al.* 2015. Novel evidence for within-species leaf economics spectrum at multiple spatial scales. *Frontiers in Plant Science* 6.

Hussner A, Hoelken HP, Jahns P. 2010. Low light acclimated submerged freshwater plants show a pronounced sensitivity to increasing irradiances. *Aquatic Botany* 93: 17–24.

Jeppesen E, Søndergaard M, Søndergaard M, Christoffersen K (Eds.). 1998. *The Structuring Role of Submerged Macrophytes in Lakes*. New York, NY: Springer New York.

Ji W, LaZerte SE, Waterway MJ, Lechowicz MJ. 2020. Functional ecology of congeneric variation in the leaf economics spectrum. *New Phytologist* 225: 196–208.

Keddy PA, Fraser LH, Solomeshch AI, Junk WJ, Campbell DR, Arroyo MTK, Alho CJR. 2009. Wet and Wonderful: The World's Largest Wetlands Are Conservation Priorities. *BioScience* 59: 39–51.

Kitajima K, Hogan KP. 2003. Increases of chlorophyll a/b ratios during acclimation of tropical woody seedlings to nitrogen limitation and high light. *Plant, Cell and Environment* 26: 857–865.

Klančnik K, Gaberščik A. 2016. Leaf spectral signatures differ in plant species colonizing habitats along a hydrological gradient. *Journal of Plant Ecology* 9: 442–450.

van Kleunen M, Weber E, Fischer M. 2010. A meta-analysis of trait differences between invasive and non-invasive plant species. *Ecology Letters* 13: 235–245.

Kokaly RF. 2001. Investigating a Physical Basis for Spectroscopic Estimates of Leaf Nitrogen Concentration. *Remote Sensing of Environment* 75: 153–161.

Kokaly RF, Asner GP, Ollinger SV, Martin ME, Wessman CA. 2009. Characterizing canopy biochemistry from imaging spectroscopy and its application to ecosystem studies. *Remote Sensing of Environment* 113: S78–S91.

Korponai J, Braun M, Buczkó K, Gyulai I, Forró L, Nédli J, Papp I. 2010. Transition from shallow lake to a wetland: a multi-proxy case study in Zalavári Pond, Lake Balaton, Hungary. *Hydrobiologia* 641: 225–244.

Kumordzi BB, Wardle DA, Freschet GT. 2015. Plant assemblages do not respond homogenously to local variation in environmental conditions: functional responses differ with species identity and abundance (A Prinzing, Ed.). *Journal of Vegetation Science* 26: 32–45.

Kunii H, Aramaki M. 1992. Annual net production and life span of floating leaves in Nymphaea tetragona Georgi: a comparison with other floating-leaved macrophytes. *Hydrobiologia* 242: 185–193.

Le Maire G, Francois C, Soudani K, Berveiller D, Pontailler J, Breda N, Genet H, Davi H, Dufrene E. 2008. Calibration and validation of hyperspectral indices for the estimation of broadleaved forest leaf chlorophyll content, leaf mass per area, leaf area index and leaf canopy biomass. *Remote Sensing of Environment* 112: 3846–3864.

Levizou E, Drilias P, Psaras GK, Manetas Y. 2004. Nondestructive assessment of leaf chemistry and physiology through spectral reflectance measurements may be misleading when changes in trichome density co-occur. *New Phytologist* 165: 463–472.

Li D, Wang X, Zheng H, Zhou K, Yao X, Tian Y, Zhu Y, Cao W, Cheng T. 2018. Estimation of area- and mass-based leaf nitrogen contents of wheat and rice crops from water-removed spectra using continuous wavelet analysis. *Plant Methods* 14: 76.

Loreau M, Hector A. 2001. Partitioning selection and complementarity in biodiversity experiments. *Nature* 412: 72–76.

Meacham-Hensold K, Fu P, Wu J, Serbin S, Montes CM, Ainsworth E, Guan K, Dracup E, Pederson T, Driever S, *et al.* 2020. Plot-level rapid screening for photosynthetic parameters using proximal hyperspectral imaging (T Lawson, Ed.). *Journal of Experimental Botany* 71: 2312–2328.

Messier J, McGill BJ, Lechowicz MJ. 2010. How do traits vary across ecological scales? A case for trait-based ecology: How do traits vary across ecological scales? *Ecology Letters* 13: 838–848.

Mevik B-H, Wehrens R. 2007. The pls Package: Principal Component and Partial Least Squares Regression in *R*. *Journal of Statistical Software* 18.

Mitra S, Wassmann R, Vlek PLG. 2005. An appraisal of global wetland area and its organic carbon stock. *Current Science* 88: 25–35.

Mitsch WJ, Bernal B, Nahlik AM, Mander Ü, Zhang L, Anderson CJ, Jørgensen SE, Brix H. 2013. Wetlands, carbon, and climate change. *Landscape Ecology* 28: 583–597.

Niinemets Ü. 2015. Is there a species spectrum within the world-wide leaf economics spectrum? Major variations in leaf functional traits in the Mediterranean sclerophyll *Quercus ilex*. *New Phytologist* 205: 79–96.

Onoda Y, Wright IJ, Evans JR, Hikosaka K, Kitajima K, Niinemets Ü, Poorter H, Tosens T, Westoby M. 2017. Physiological and structural tradeoffs underlying the leaf economics spectrum. *New Phytologist* 214: 1447–1463.

Osnas JLD, Katabuchi M, Kitajima K, Wright SJ, Reich PB, Van Bael SA, Kraft NJB, Samaniego MJ, Pacala SW, Lichstein JW. 2018. Divergent drivers of leaf trait variation within species, among species, and among functional groups. *Proceedings of the National Academy of Sciences* 115: 5480–5485.

Peterson RB, Oja V, Laisk A. 2001. Chlorophyll fluorescence at 680 and 730 nm and leaf photosynthesis. *Photosynthesis Research* 70: 185–196.

Pinardi M, Bartoli M, Longhi D, Viaroli P. 2011. Net autotrophy in a fluvial lake: the relative role of phytoplankton and floating-leaved macrophytes. *Aquatic Sciences* 73: 389–403.

Poorter H, Niinemets Ü, Poorter L, Wright IJ, Villar R. 2009. Causes and consequences of variation in leaf mass per area (LMA): a meta-analysis. *New Phytologist* 182: 565–588.

Sandel B, Low R. 2019. Intraspecific trait variation, functional turnover and trait differences among native and exotic grasses along a precipitation gradient (Z Botta-Dukát, Ed.). *Journal of Vegetation Science* 30: 633–643.

Santamaría L. 2002. Why are most aquatic plants widely distributed? Dispersal, clonal growth and small-scale heterogeneity in a stressful environment. *Acta Oecologica* 23: 137–154.

Schaepman ME, Jehle M, Hueni A, D'Odorico P, Damm A, Weyermann J, Schneider FD, Laurent V, Popp C, Seidel FC, *et al.* 2015. Advanced radiometry measurements and Earth science applications with the Airborne Prism Experiment (APEX). *Remote Sensing of Environment* 158: 207–219.

Schindler DE, Scheuerell MD. 2002. Habitat coupling in lake ecosystems. *Oikos* 98: 177–189.

Schweiger AK, Schütz M, Risch AC, Kneubühler M, Haller R, Schaepman ME. 2017. How to predict plant functional types using imaging spectroscopy: linking vegetation community traits, plant functional types and spectral response (R Chisholm, Ed.). *Methods in Ecology and Evolution* 8: 86–95.

Serbin SP, Wu J, Ely KS, Kruger EL, Townsend PA, Meng R, Wolfe BT, Chlus A, Wang Z, Rogers A. 2019. From the Arctic to the tropics: multibiome prediction of leaf mass per area using leaf reflectance. *New Phytologist* 224: 1557–1568.

Sims DA, Gamon JA. 2002. Relationships between leaf pigment content and spectral reflectance across a wide range of species, leaf structures and developmental stages. *Remote Sensing of Environment* 81: 337–354.

Singh A, Serbin SP, McNeil BE, Kingdon CC, Townsend PA. 2015. Imaging spectroscopy algorithms for mapping canopy foliar chemical and morphological traits and their uncertainties. *Ecological Applications* 25: 2180–2197.

Smith WK, Vogelmann TC, DeLucia EH, Bell DT, Shepherd KA. 1997. Leaf Form and Photosynthesis. *BioScience* 47: 785–793.

Søndergaard M, Johansson LS, Lauridsen TL, Jørgensen TB, Liboriussen L, Jeppesen E. 2010. Submerged macrophytes as indicators of the ecological quality of lakes. *Freshwater Biology* 55: 893–908.

Spence DHN. 1982. The Zonation of Plants in Freshwater Lakes. In: Macfadyen A, Ford ED, eds. Advances in Ecological Research. Academic Press, 37–125.

Stratoulias D, Balzter H, Zlinszky A, Tóth VR. 2015. Assessment of ecophysiology of lake shore reed vegetation based on chlorophyll fluorescence, field spectroscopy and hyperspectral airborne imagery. *Remote Sensing of Environment* 157: 72–84.

Stratoulias D, Tóth VR. 2020. Photophysiology and Spectroscopy of Sun and Shade Leaves of Phragmites australis and the Effect on Patches of Different Densities. *Remote Sensing* 12: 200.

Terashima I, Hikosaka K. 1995. Comparative ecophysiology of leaf and canopy photosynthesis. *Plant, Cell and Environment* 18: 1111–1128.

Thomaz Sm, Carvalho P, Padial Aa, Kobayashi Jt. 2009. Temporal and spatial patterns of aquatic macrophyte diversity in the Upper Paraná River floodplain. *Brazilian Journal of Biology* 69: 617–625.

Tóth VR, Szabó K. 2012. Morphometric structural analysis of *Phragmites australis* stands in Lake Balaton. *Annales de Limnologie - International Journal of Limnology* 48: 241–251.

Tóth VR, Vári Á. 2013. Impact of habitat environment on *Potamogeton perfoliatus* L. morphology and its within-plant variability in Lake Balaton. *Annales de Limnologie - International Journal of Limnology* 49: 149–155.

Tóth VR, Palmer SCJ. 2016. Acclimation of Potamogeton perfoliatus L. to periphyton accumulation-induced spectral changes in irradiance. *Hydrobiologia* 766: 293–304.

Tóth VR. 2018. Monitoring Spatial Variability and Temporal Dynamics of Phragmites Using Unmanned Aerial Vehicles. *Frontiers in Plant Science* 9: 728.

Tóth VR, Villa P, Pinardi M, Bresciani M. 2019. Aspects of Invasiveness of Ludwigia and Nelumbo in Shallow Temperate Fluvial Lakes. *Frontiers in Plant Science* 10: 647.

Tranvik LJ, Downing JA, Cotner JB, Loiselle SA, Striegl RG, Ballatore TJ, Dillon P, Finlay K, Fortino K, Knoll LB, *et al.* 2009. Lakes and reservoirs as regulators of carbon cycling and climate. *Limnology and Oceanography* 54: 2298–2314.

Turak E, Harrison I, Dudgeon D, Abell R, Bush A, Darwall W, Finlayson CM, Ferrier S, Freyhof J, Hermoso V, *et al.* 2017. Essential Biodiversity Variables for measuring change in global freshwater biodiversity. *Biological Conservation* 213: 272–279.

Ustin SL, Gitelson AA, Jacquemoud S, Schaepman M, Asner GP, Gamon JA, Zarco-Tejada P. 2009. Retrieval of foliar information about plant pigment systems from high resolution spectroscopy. *Remote Sensing of Environment* 113: S67–S77.

Verrelst J, Camps-Valls G, Muñoz-Marí J, Rivera JP, Veroustraete F, Clevers JGPW, Moreno J. 2015. Optical remote sensing and the retrieval of terrestrial vegetation bio-geophysical properties – A review. *ISPRS Journal of Photogrammetry and Remote Sensing* 108: 273–290.

Villa P, Bresciani M, Bolpagni R, Pinardi M, Giardino C. 2015. A rule-based approach for mapping macrophyte communities using multi-temporal aquatic vegetation indices. *Remote Sensing of Environment* 171: 218–233.

Villa P, Pinardi M, Tóth VR, Hunter PD, Bolpagni R, Bresciani M. 2017. Remote sensing of macrophyte morphological traits: implications for the management of shallow lakes. *Journal of Limnology*.

Villa P, Pinardi M, Bolpagni R, Gillier J-M, Zinke P, Nedelcuţ F, Bresciani M. 2018. Assessing macrophyte seasonal dynamics using dense time series of medium resolution satellite data. *Remote Sensing of Environment* 216: 230–244.

Vivian-Smith G. 1997. Microtopographic Heterogeneity and Floristic Diversity in Experimental Wetland Communities. *The Journal of Ecology* 85: 71.

Wang Q, Li P. 2012. Hyperspectral indices for estimating leaf biochemical properties in temperate deciduous forests: Comparison of simulated and measured reflectance data sets. *Ecological Indicators* 14: 56–65.

Wang W, Fraser JD, Chen J. 2019. Distribution and Long-Term Population Trends of Wintering Waterbirds in Poyang Lake, China. *Wetlands* 39: 125–135.

Wang R, Gamon JA. 2019. Remote sensing of terrestrial plant biodiversity. *Remote Sensing of Environment* 231: 111218.

Wetzel RG. 1990. Land-water interfaces: Metabolic and limnological regulators. *SIL Proceedings, 1922-2010* 24: 6–24.

Wold S, Sjöström M, Eriksson L. 2001. PLS-regression: a basic tool of chemometrics. *Chemometrics and Intelligent Laboratory Systems* 58: 109–130.

Wright IJ, Reich PB, Westoby M, Ackerly DD, Baruch Z, Bongers F, Cavender-Bares J, Chapin T, Cornelissen JHC, Diemer M, *et al.* 2004. The worldwide leaf economics spectrum. *Nature* 428: 821–827.

Wu J, Chavana-Bryant C, Prohaska N, Serbin SP, Guan K, Albert LP, Yang X, van Leeuwen WJD, Garnello AJ, Martins G, *et al.* 2017. Convergence in relationships between leaf traits, spectra and age across diverse canopy environments and two contrasting tropical forests. *New Phytologist* 214: 1033–1048.

Yao X, Zhu Y, Tian Y, Feng W, Cao W. 2010. Exploring hyperspectral bands and estimation indices for leaf nitrogen accumulation in wheat. *International Journal of Applied Earth Observation and Geoinformation* 12: 89–100.